Supporting Information

Table S1: Hydroxyl content and molecular weight of lignin precursors.

Sample	Aliphatic - OH (mmol/g)	Aromatic -OH (mmol/g)	Carboxylic Acid (mmol/g)	Total OH Content (mmol/g)	Mw	Mn	PDI
Kraft Lignin	2.05	3.53	0.51	6.11	16,558	5,142	3.2
Oxyalkylated	4.73	0	0	4.73	10,400	2,911	3.6
Cyclocarbonated	1.51	0	0	1.51	14,023	3,396	4.1

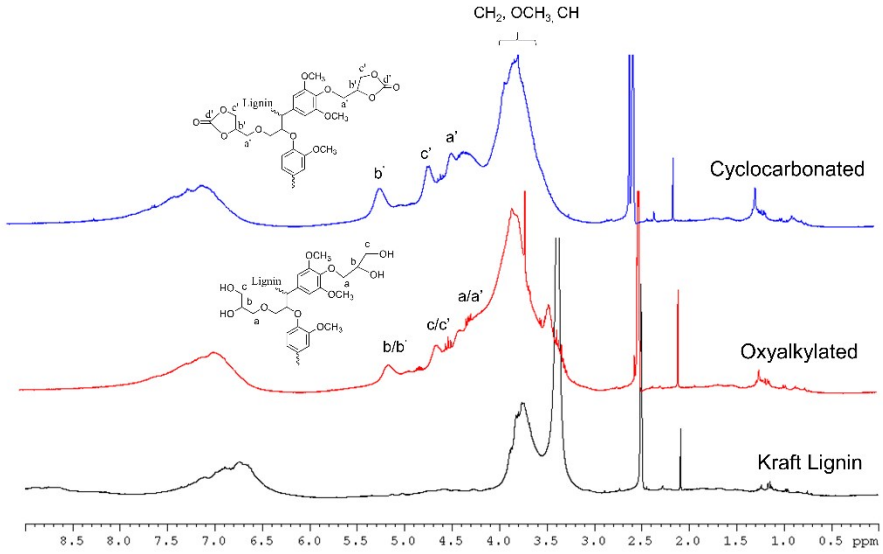

Figure S1: ^{1}H NMR of lignin after the reaction with glycerol carbonate (oxyalklyated) and the subsequent reaction with dimethyl carbonate (cyclocarbonated). The appearance of the sharp peak at 3.5 ppm results from the addition of the methylene groups of oxyalkylated strands while the peaks from 4-5 ppm refer to protons in the cyclocarbonate ring.

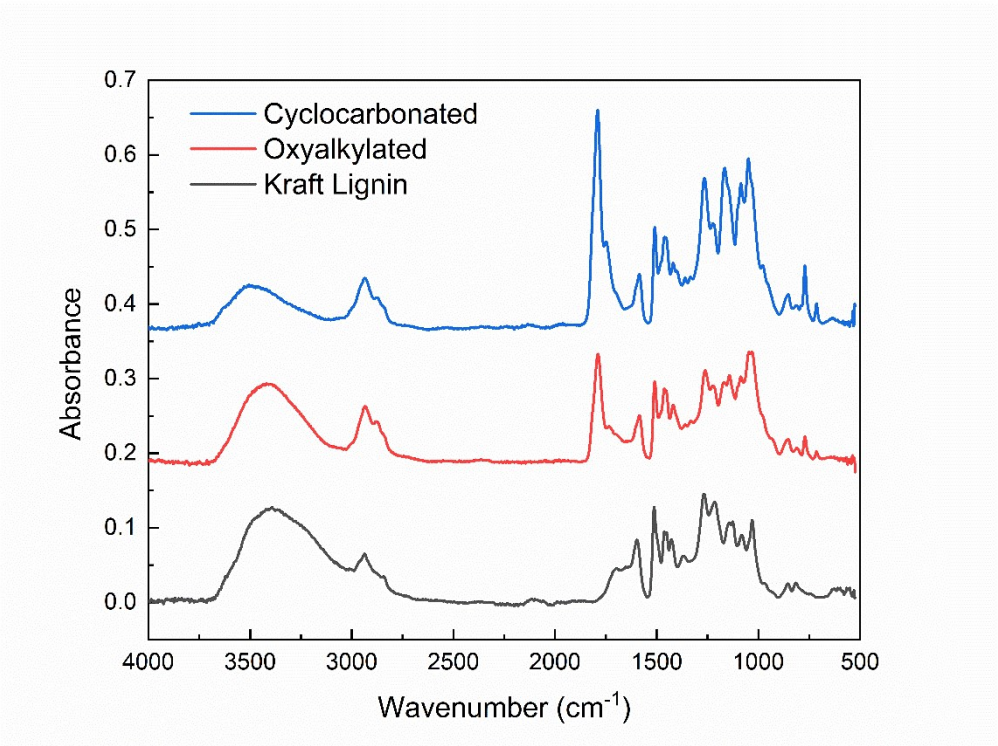

Figure S2: FTIR of functionalized lignin precursors. The functionalization of Kraft lignin with glycerol carbonate (oxyalkylated) creates an increase in signal intensity corresponding to the C-O stretching (1000 – 1100 cm^{-1}) of etherified strands as well as increased signals in the carbonyl region reflecting both the presence of linear and cyclocarbonates (1700 , 1795 cm^{-1} respectively). A subsequent reaction with dimethyl carbonate produces a noticeable increase in the cyclocarbonate peak as a result of a ring-closing transesterification reaction.

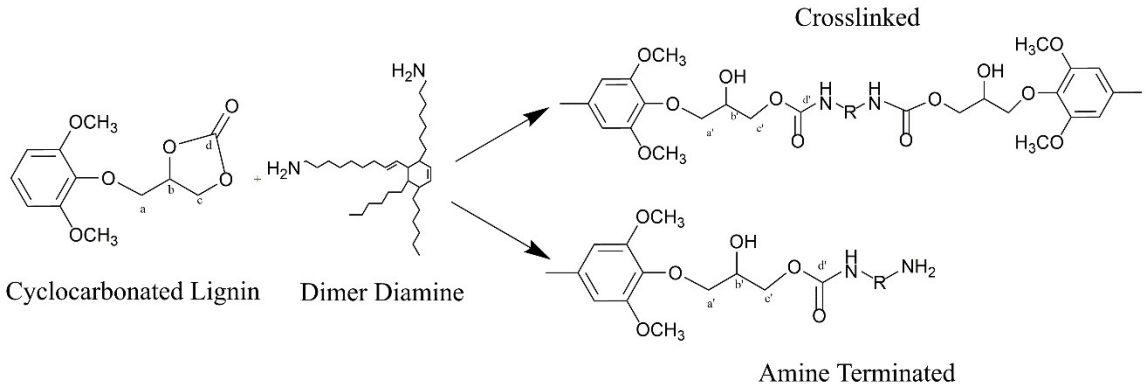

Figure S3: Two pathways for the reaction of the dimer diamine with cyclocarbonated lignin. Stoichiometric reaction mixtures will favor crosslinked structures whereas an excess of diamine will lead to amine terminated moieties.

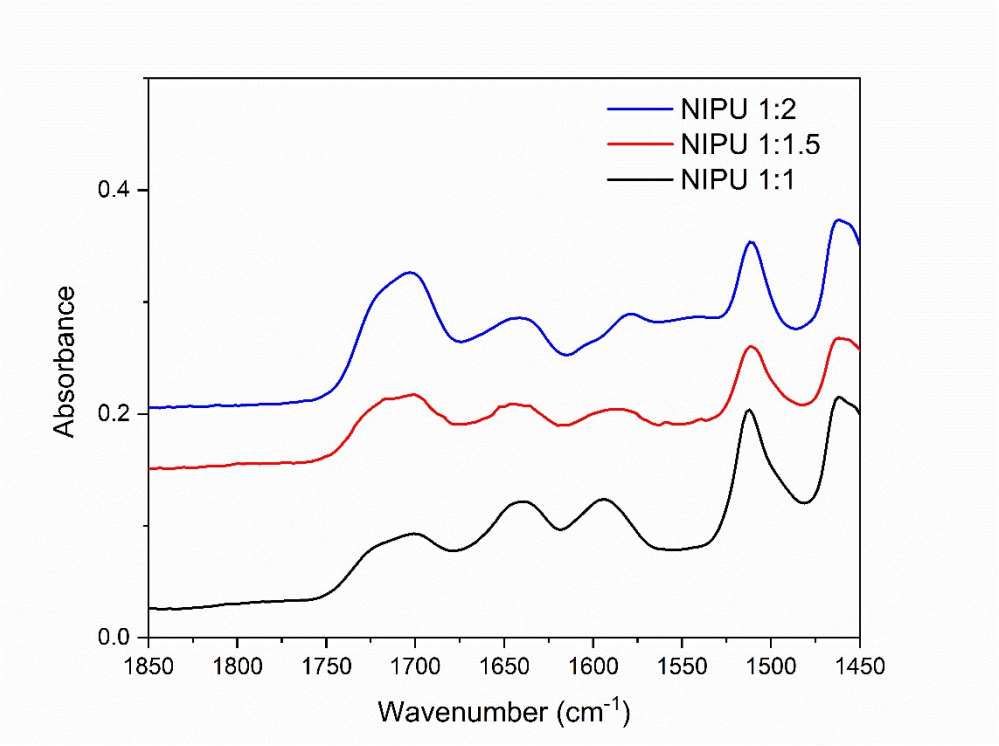

Figure S4 : Expanded view of the carbonyl and aromatic region of NIPU samples of varying reaction stoichiometry. All samples show a complete disappearance of the cyclocarbonate peak at 1795 cm^{-1} in favor of urethane and urea peaks at 1720 cm^{-1} and 1650 cm^{-1} respectively.

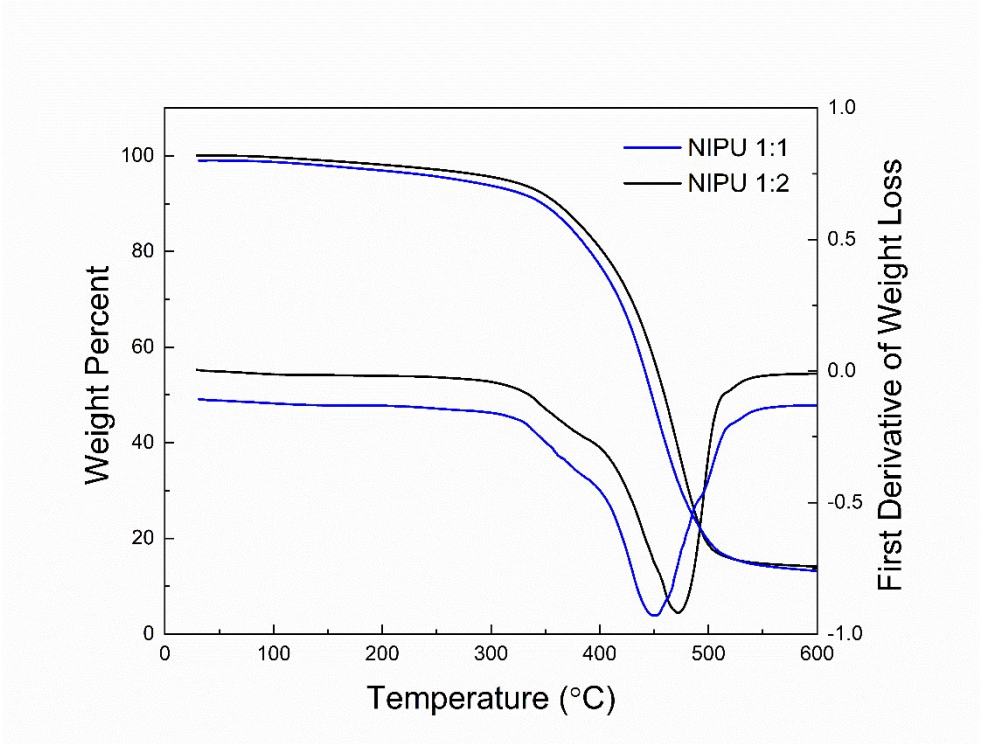

Figure S5: Thermogravimetric analysis of NIPU 1:1 and NIPU 1:2. A two step degradation mechanism is seen by the disassociation of urethane bonds at 350°C and further degradation of the lignin and diamine constituents thereafter.

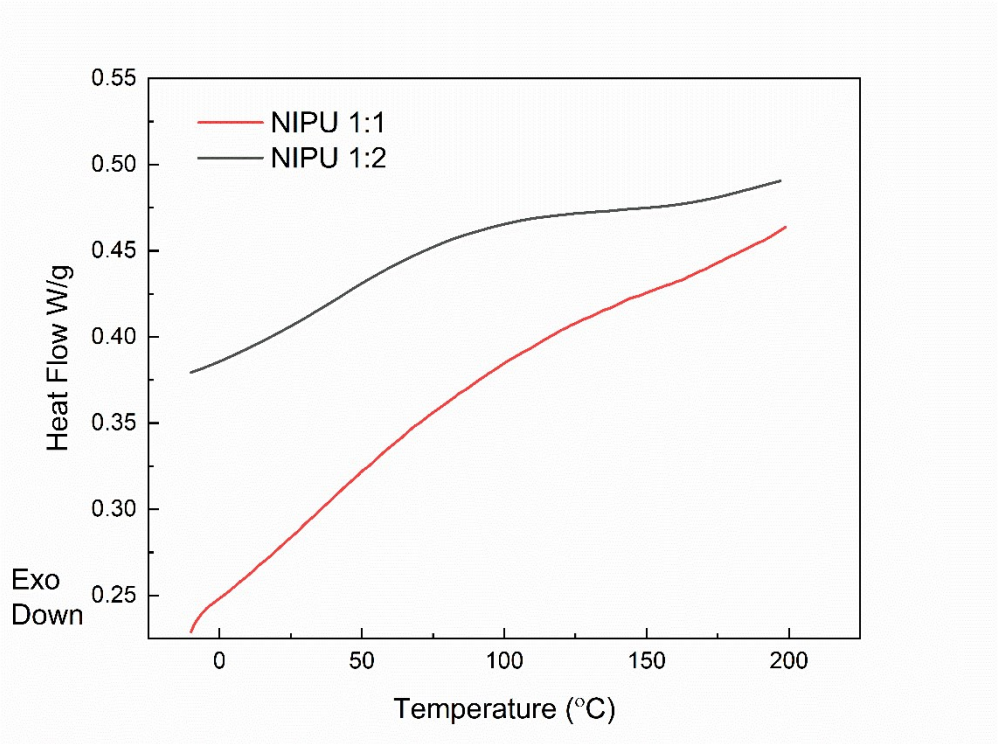

Figure S6: DSC thermograms of the second heating cycle for NIPU 1:1 and NIPU 1:2. A broad transition region from the glassy state is observed for NIPU 1:2 while the increased crosslinking density in NIPU 1:1 exhibits a smaller transition.

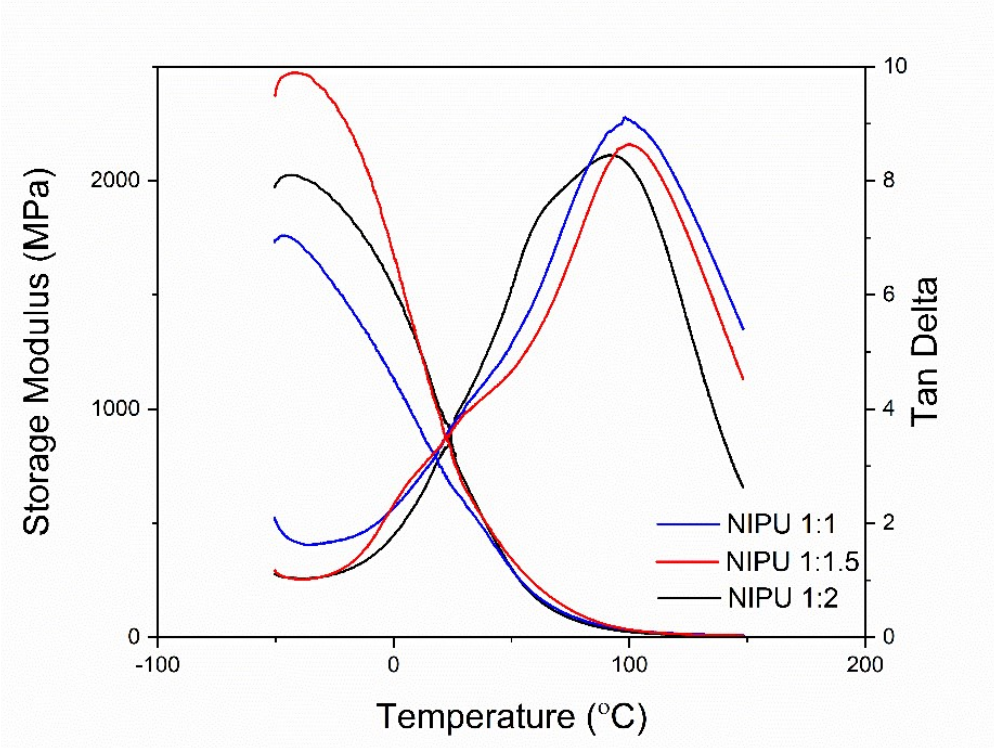

Figure S7: Dynamic mechanical analysis of NIPU samples showing Storage Modulus and Tan Delta curves. The alpha relaxation temperature is seen to decrease and broaden with increasing soft segment incorporation from NIPU 1:1 to NIPU 1:2.